Robotica (2011) volume 29, pp. 939–947. © Cambridge University Press 2011
doi:10.1017/S0263574711000166

Heuristic control of bipedal running: steady-state and accelerated†

A. D. Perkins*, K. J. Waldron and P. J. Csonka

Robotic Locomotion Laboratory, Mechanical Engineering Department, Stanford University, Stanford, CA 94305, USA. E-mails: {kwaldron,pcsonka}@stanford.edu

(Received in Final Form: February 8, 2011. First published online: March 15, 2011)

SUMMARY

The design, control, and actuation of legged robots that walk is well established, but there remain unsolved problems for legged robots that run. In this work, dynamic principles are used to develop a set of heuristics for controlling bipedal running and acceleration. These heuristics are then converted into control laws for two very different bipedal systems: one with a high-inertia torso and prismatic knees and one with a low-inertia torso, articulated knees, and mechanical coupling between the knee and ankle joints. These control laws are implemented in simulation to achieve stable steady-state running, accelerating, and decelerating. Stable steady-state running is also achieved in a planar experimental system with a semiconstrained torso.

KEYWORDS: Control of robotic systems; Legged robots; Bipeds; Biomimetic robots; Robot dynamics.

1. Introduction

There are a great variety of applications that would benefit from bipedal robotic workers, including military transport through rugged terrain and search and rescue amidst debris. To date, no robotic systems have been created that have dynamic maneuvering capabilities robust enough to be functional in these situations. There are some, like the 230 g, 160 mm SPRAWL,[1] which maneuver well but are too small to be practically useful. Others, like Raibert's biped,[2] perform dynamic runs and aerial maneuvers, but require very specific system parameters that render them ineffective for general applications. Still others, like Boston Dynamics' BigDog[3] and Honda's ASIMO,[4] are large and robust but are not designed for high-speed locomotion.

There is a good reason why natural systems run at high speeds: it is more energetically efficient than walking. As the desired rate of travel increases, it eventually becomes more metabolically efficient to shorten the stance period of each foot enough that a flight phase appears.[5] This can be shown to be true for robotic legged systems as well, using mechanical work in place of metabolic work. While robots like ASIMO have technically "run"—that is, they have achieved distinct flight phases—they have done so for the sake of running, not for the sake of dynamic efficiency.

The goal of the work presented here is to develop control strategies that allow a robot of human proportions to perform two of the most basic dynamic maneuvers witnessed in nature: steady-state running and acceleration. A set of heuristics is developed on the basis of dynamical principles and physical intuition. Given a specific system, these can be converted into control laws. This is done for two different systems: a prismatic legged system with human mass distribution and an articulated legged system with a relatively lower inertia torso and mechanical coupling between the ankle and knee joints. Despite the differences in these two systems, the same set of heuristics produces stable results in simulations of both, successfully executing stable steady-state running and both slow-rate and high-rate acceleration in both systems.

2. Control Philosophy

In the field of legged robotics, there are several different control philosophies that have been successfully implemented on various systems. One approach is *model-based control*, which relies on high-fidelity dynamic models of the robotic system under study. These models are used to create control laws through a variety of modern control techniques, such as feed-back linearization, which can be analytically studied and optimized.[6] However, these control laws are most effective when the dynamic models on which they are based are extremely accurate; thus, significant system identification is required, and small design changes can have large repercussions in control design. A second control approach is *machine learning* (e.g., genetic algorithms, fuzzy control, supervised/unsupervised learning). These techniques can lead to highly optimized algorithms and are particularly useful for tuning gains.[7] However, they generally require high-fidelity models or relatively accurate seeds and large amounts of data collected during expensive experimental trials. In any legged system conducting dynamic maneuvers, each experimental trial corresponds to many large impacts and high wear on components, which is not desirable for prototype systems. A third control strategy is the use of *central pattern generators* (CPGs), which use a repetitive pattern of commands to produce a gait and are inspired by biologic systems that use repetitive impulses from the peripheral nervous system, not the central nervous system, to control most gaits. CPGs require little computational power and have reduced dependency on high-accuracy or high-bandwidth sensors[8] and can produce highly efficient gaits.[9] Unfortunately,

†This paper was originally submitted under the auspices of the CLAWAR Association. It is an extension of work presented at CLAWAR 2009: The 12th International Conference on Climbing and Walking Robots and the Support Technologies for Mobile Machines, Istanbul, Turkey.

†Corresponding author. E-mail: alexp2@stanford.edu

because CPGs are largely feed forward, they are much less robust to disturbances than other methods of control.

Another approach to controlling legged robotics is *heuristic control*, which requires a relatively simple dynamic model of the system. This model is used to develop a set of heuristics, or rules, which can then be translated into joint-specific control laws.[2] Heuristic control generally does not produce provably stable control laws, as model-based control does, nor does it produce optimal performance like machine learning, and it requires much higher computational power than CPGs. However, it is less sensitive to model inaccuracies than model-based control, does not require large training sets of data to produce stable results like machine learning, and is more robust to disturbances than CPGs. In addition, heuristic control is derived from intuition, common sense, and simple laws of physics, making it easier to develop and diagnose. Thus, the controller presented in this work is a heuristic controller, with the heuristics presented below and the actual control laws presented in Section 3.

It is worth noting that the model of the system can be quite general. For the work presented here, it is assumed that the system being controlled holds to a few loose requirements: it is bipedal and symmetric about the sagittal plane, it has articulated hips connecting a torso to the legs, and the hips and the knees are fully actuated. Rotation about the lateral, longitudinal, and vertical axes are called "pitch," "roll," and "yaw," respectively. All axes listed here are in the machine frame. The angle of a leg with the vertical in the pitch plane is called "swing," and the angle of a leg with the vertical in roll plane is called "spread". "Foot-strike" refers to the instant at which the foot first comes into contact with the ground and "toe-off" refers to the instant at which the foot completely leaves contact with the ground.

In order to develop appropriate heuristics, the dynamics of a legged mechanism with a flight phase must be considered. This is frequently done using the SLIP model.[10] However, the SLIP model has no closed form solution. As an alternative, Abdallah and Waldron[11] suggested a stance model that considers the net vertical and horizontal impulses on the body over the entire stance, which is used as the base of the work presented here. Abdallah's work is based on assumptions of a symmetric stance and a constant leg thrust. A symmetric stance is characterized by the leg length being equal at foot-strike and toe-off and the leg angle at foot-strike being opposite across the vertical from the leg angle at toe-off.

To appropriately handle velocity errors and disturbances, feedback is necessary. The feedback proposed here involves adjusting three parameters: the leg swing angle at foot-strike $\alpha_{\text{hip}}^{\text{fs}}$, the leg spread angle at foot-strike $\beta_{\text{hip}}^{\text{fs}}$, and the virtual leg length $\ell_{\text{leg}}^{\text{to}}$ at which thrust in the leg is ceased, thereby causing toe-off. Alternately, the leg swing angle $\alpha_{\text{hip}}^{\text{to}}$ could be used to determine when to end the leg thrust and terminate ground contact; the selection of controlling $\ell_{\text{leg}}^{\text{to}}$ is completely arbitrary.

2.1. Heuristics

The first set of heuristics developed are for steady-state running, which for this work translates to moving forward at a near constant velocity with little lateral displacement. Obviously, the forward velocity and lateral position will change over the course of a stride, but their values at the start of consecutive strides should not change. Thus, steady-state running is characterized by stable limit cycles in many system parameters, such as vertical or lateral displacement of the system center of mass (COM).[12] As each steady-state heuristic is developed, its applicability to accelerating is considered, and it is either kept or modified as necessary.

Given an approximately symmetric leg thrust and stance, the net impulse on the system over the entire stance will be vertical. In order to minimize the pitch impulse on the torso, the net vertical impulse should pass through the torso COM. This is expressed in the first heuristic:

SS.1 *Keep the torso upright,*

which is equally applicable for accelerating,

AC.1 *Keep the torso upright.*

Typically, the hip actuators of a legged robot are used in flight to position the legs for touchdown, sacrificing some torso pitch in the process. However, if the torso inertia is low relative to the leg inertia, any attempt to posture the legs will result in immediate and severe pitching of the torso while hardly moving the leg at all. Because the heuristics should be general rules applicable to a wide variety of systems, it is conservative to assume a low inertia torso which cannot be relied upon to posture the legs during flight. However, there is another object in the system of approximately equal inertia to the leg being positioned: the other leg. Thus,

SS.2 *Position extending leg using retracting leg,*

which is equally applicable for accelerating,

AC.2 *Position extending leg using retracting leg.*

The next consideration applies only to 3D (nonplanar) robotic systems and involves controlling the lateral velocity:

SS.3 *If drifting left, place next foot farther left, and* vice versa*,*

which is equally applicable for accelerating,

AC.3 *If drifting left, place next foot farther left, and* vice versa*.*

Similarly, if the forward velocity is greater than desired, a net rearward impulse can be generated by placing the foot farther ahead at foot-strike to "brake" the robot:

SS.4 *To slow down, place next foot farther forward, and* vice versa*.*

This can be taken to an extreme for accelerating:

AC.4 *Place foot under hip at foot-strike.*

If the vertical velocity is less than desired, a net vertical impulse greater than $2\,m\,v_z$ can be generated by lengthening the duration of the contact, which implies:

SS.5 *To hop higher, increase stance duration, and* vice versa*.*

However, this heuristic cannot be taken too far, as the leg has a finite length. Thus, it is necessary to retract the leg more than normal in anticipation of acceleration, allowing a longer impulse:

https://doi.org/10.1017/S0263574711000166 Published online by Cambridge University Press

AC.5 *Decrease effective leg length at foot-strike.*

Finally, there is a coupling between the touchdown angle and release leg length, because each effects the parameter that the other is meant to control. By shifting the touchdown angle, a nonzero net horizontal impulse is introduced at the expense of decreasing the vertical impulse, regardless of which way the foot-strike angle is shifted. This can be compensated for by the final heuristic:

SS.6 *If wrong speed, increase stance duration.*

For acceleration, there is clearly a large forward velocity error. Thus, the stance should be increased as long as possible to maximize the energy addition:

AC.6 *Thrust as long as possible.*

This set of heuristics is sufficient for steady-state running. However, acceleration is an inherently paired process: if acceleration is only carried out over a single stride, then a yaw rate will be permanently induced, which causes turning. To prevent this, the next stride must provide an equal forward impulse, so that the yaw rate induced by the first stride is negated. In biologic systems, it is possible to overcome this by applying a moment about the leg axis, but many robotic systems are unable to impart such a moment. Thus, an extra accelerating heuristic is necessary:

AC.7 *Execute the same process over two consecutive stances.*

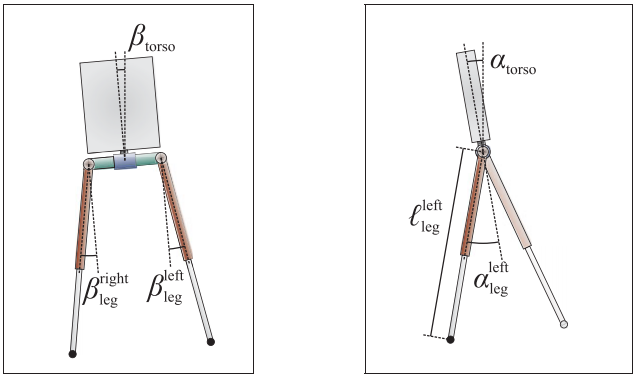

Fig. 1. The first simulated system: a prismatic legged system with 13 DOF (7 actuated), showing (a) the front view (forward motion out of the page) and (b) the side view (forward motion to the left). As shown, $\beta_{\text{pelvis}} > 0$, $\beta_{\text{hip}}^{\text{right}} > 0$, $\beta_{\text{hip}}^{\text{left}} > 0$, $\alpha_{\text{torso}} > 0$, and $\alpha_{\text{hip}}^{\text{left}} < 0$.

Table I. Model parameters for the first simulated system, which are taken from Leva to be approximately human in both size and mass.

Link	Length (m)	Mass (kg)	Inertia (kg/m^2) (lateral, longitudinal, vertical)
Torso	0.6	48	15, 8, 8
Thigh	0.5	1.4	1, 1, 0.1
Shank	0.5	–	–
Foot	–	0.5	–

3. Control Laws

In order to convert the heuristics presented in Section 2.1 into actual control laws, it is necessary to determine the system being controlled. This points to one of the strengths of heuristic control: the heuristics are applicable to a wide range of systems, regardless of specific architecture. To demonstrate this, the heuristics developed in Section 2.1 are tested in simulation on two very different bipeds. The first is a prismatic legged system with 13 degrees of freedom (DOFs), point feet, no ankle, and approximately human mass distribution. The second is an articulated legged system with 17 DOFs, nonpoint feet, a tendon coupling between the ankle and knee joints, and a relatively low inertia torso.

3.1. Prismatic legged system

The first system is shown in Fig. 1. This system has 13 total DOFs, of which 3 are for the position of the hip axis, 2 are for the orientation of the hip axis, 2 are for the orientation of the torso, and the remaining 6 are for the orientation and position of the legs' segments. These are detailed here, again with all axes listed in the machine frame. There are three unactuated translational DOFs that describe the position of the center of the hip axis and two unactuated rotational DOFs that describe the orientation of the hip axis with respect to a global reference about the vertical and longitudinal axes. Additionally, there is one unactuated rotational DOF that describes the orientation of the torso with respect to a global reference about the lateral axis and one actively actuated rotational DOF that describes the orientation of the torso with respect to the hip axis about the vertical axis. Finally, there are three DOFs in each leg: one actively actuated rotational DOF that describes the orientation of the thigh with respect to the torso about the lateral axis, one actively actuated rotational DOF that describes the orientation of the thigh with respect to the hip axis about the longitudinal axis, and one actively actuated translational DOF that describes the position of the foot with respect to the knee along the vertical thigh axis. The link sizes were selected to match human proportions given in Leva[13] and are detailed in Table I.

3.1.1. Steady-state. For the results presented in Section 4, the leg thrust was selected on the basis of Abdallah's model and was kept constant over any particular stance. Defining the forward and lateral velocity errors $\mathrm{v}_{\mathrm{F}}^{\mathrm{err}}$ and $\mathrm{v}_{\mathrm{L}}^{\mathrm{err}}$ and hopping height error $\mathrm{p}_{\mathrm{Z}}^{\mathrm{err}}$ as

$$\mathrm{v}_{\mathrm{F}}^{\mathrm{err}} \triangleq \left(\mathrm{v}_{\mathrm{F}}^{\mathrm{des}} - \mathrm{v}_{\mathrm{F}}^{\mathrm{act}}\right)\left(\mathrm{v}_{\mathrm{F}}^{\mathrm{des}}\right)^{-1}, \tag{1}$$

$$\mathrm{v}_{\mathrm{L}}^{\mathrm{err}} \triangleq \left(\mathrm{v}_{\mathrm{L}}^{\mathrm{des}} - \mathrm{v}_{\mathrm{L}}^{\mathrm{act}}\right)\left(\mathrm{v}_{\mathrm{L}}^{\mathrm{des}}\right)^{-1}, \tag{2}$$

$$\mathrm{p}_{\mathrm{Z}}^{\mathrm{err}} \triangleq \left(\mathrm{p}_{\mathrm{Z}}^{\mathrm{des}} - \mathrm{p}_{\mathrm{Z}}^{\mathrm{act}}\right)\left(\mathrm{p}_{\mathrm{Z}}^{\mathrm{des}}\right)^{-1}, \tag{3}$$

where $\mathrm{v}_{\mathrm{F}}^{\mathrm{des}}$ and $\mathrm{v}_{\mathrm{F}}^{\mathrm{act}}$ are the desired and actual forward velocities, $\mathrm{v}_{\mathrm{L}}^{\mathrm{des}}$ and $\mathrm{v}_{\mathrm{L}}^{\mathrm{act}}$ are the desired and actual lateral velocities, and $\mathrm{p}_{\mathrm{Z}}^{\mathrm{des}}$ and $\mathrm{p}_{\mathrm{Z}}^{\mathrm{act}}$ are the desired and actual hop heights. Using Eqs. (1)–(3) allows heuristics SS.4–SS.6 to be combined with proportional control to produce

$$\alpha_{\text{hip}}^{\text{fs}} = \alpha_{\text{hip}}^{\text{nom}}\left(1 + k_{sw}^{\mathrm{F}}\mathrm{v}_{\mathrm{F}}^{\mathrm{err}} - k_{sw}^{\mathrm{Z}}\mathrm{p}_{\mathrm{Z}}^{\mathrm{err}}\right), \tag{4}$$

$$\beta_{\text{hip}}^{\text{fs}} = \beta_{\text{hip}}^{\text{nom}}\left(1 + k_{sp}^{\mathrm{L}}\mathrm{v}_{\mathrm{L}}^{\mathrm{err}}\right), \tag{5}$$

https://doi.org/10.1017/S0263574711000166 Published online by Cambridge University Press

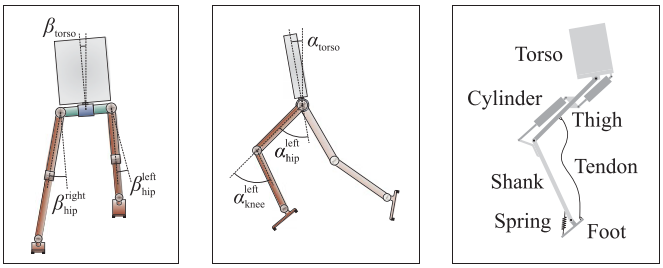

Fig. 2. The second simulated system: an articulated legged biped with 17 DOFs (7 actuated), showing (a) the front view (forward motion out of the page), (b) the side view (forward motion to the left), and (c) the actuator layout. As shown, $\beta_{\text{pelvis}} > 0$, $\beta_{\text{hip}}^{\text{right}} > 0$, and $\beta_{\text{hip}}^{\text{left}} < 0$, $\alpha_{\text{torso}} > 0$, $\alpha_{\text{hip}}^{\text{left}} < 0$, and $\alpha_{\text{knee}}^{\text{left}} < 0$.

$$l_{\text{leg}}^{\text{fs}} = l_{\text{hip}}^{\text{nom}}, \tag{6}$$

$$l_{\text{leg}}^{\text{to}} = l_{\text{hip}}^{\text{nom}} \left(1 + k_{len}^{\text{F}} \left|\text{v}_{\text{F}}^{\text{err}}\right| - k_{len}^{\text{Z}} \text{p}_{\text{Z}}^{\text{err}}\right), \tag{7}$$

where $\alpha_{\text{hip}}^{\text{nom}}$ and $\beta_{\text{hip}}^{\text{nom}}$ are some preselected leg swing and spread angles at foot-strike, $l_{\text{hip}}^{\text{nom}}$ is some preselected leg length at take off, $\alpha_{\text{hip}}^{\text{fs}}$ and $\beta_{\text{hip}}^{\text{fs}}$ are the desired leg angles at foot-strike adjusted for velocity errors, $l_{\text{leg}}^{\text{fs}}$ and $l_{\text{leg}}^{\text{to}}$ are the desired leg lengths at foot-strike and take off, and k_{param}^{dir} is proportional control gain. These adjusted parameters, as well as SS.1, can then be fed into whatever control algorithms are desired to control specific joints. For the results presented in Section 4, simple proportional-derivative control was implemented, with linear gain scheduling to allow performance over a wide operating range.

3.1.2. Acceleration. The accelerating heuristics given in Section 2.1 can also be converted into control laws. For acceleration, the equations governing the four control parameters become

$$\alpha_{\text{hip}}^{\text{fs}} = 0^{\circ}, \tag{8}$$

$$\beta_{\text{hip}}^{\text{fs}} = \beta_{\text{hip}}^{\text{nom}} \left(1 + k_{sp}^{\text{L}} \text{v}_{\text{L}}^{\text{err}}\right), \tag{9}$$

$$l_{\text{leg}}^{\text{fs}} = l_{\text{leg}}^{\text{nom}} \left(1 - k_{len}^{\text{F}} \text{v}_{\text{F}}^{\text{err}}\right), \tag{10}$$

$$l_{\text{leg}}^{\text{to}} = l_{\text{leg}}^{\text{max}}, \tag{11}$$

where $l_{\text{leg}}^{\text{max}}$ is the maximum possible leg extension. Note that Eqs. (5) and (9) are identical.

3.2. Articulated legged system

The second system is shown in Fig. 2. This system has 17 total DOFs, of which 3 are for the position of the hip axis, 2 are for the orientation of the hip axis, 2 are for the orientation of the torso, and the remaining 10 are for the orientation of the legs' segments. These are detailed here, again with all axes listed in the machine frame. There are three unactuated translational DOFs that describe the position of the center of the hip axis, and two unactuated rotational DOFs that describe the orientation of the hip axis with respect to a global reference about the vertical and longitudinal axes. Additionally, there is one unactuated rotational DOF that describes the orientation of the torso with respect to a global reference about the lateral axis and one actively actuated rotational DOF that describes the orientation of the torso with respect to the hip axis about the vertical axis. Finally, there are five DOFs in each leg: one actively actuated rotational DOF that describes the orientation of the thigh with respect to the torso about the lateral axis, one actively actuated rotational DOF that describes the orientation of the thigh with respect to the hip axis about the longitudinal axis, one actively actuated rotational DOF that describes the orientation of the shank with respect to the thigh about the lateral axis, one passively actuated rotational DOF that describes the orientation of the foot with respect to the shank about the lateral axis, and one passively actuated rotational DOF that describes the orientation of the foot with respect to the shank about the longitudinal axis.

There are three main differences between this model and the prismatic legged model presented in Section 3.1. First, the ankle joint has only passive springs and a tendon providing mechanical coupling between the ankle and knee joints. The use of a tendon and an unactuated ankle was selected primarily because placing an actuator at the ankle greatly increases the leg inertia about the hip, which is undesirable as it increases the energetic cost of running.[14] However, the ankle plays a crucial role in running,[15] so some level of control is necessary. Examining biologic systems leads to the idea of mechanical coupling between the ankle and knee, which is commonly seen in biarticular muscle/tendon groups. This is easily seen in humans: when the knee joint is straightened, it is natural to point the toe, because a tendon stretches from the buttocks to the ankle through a passage under the knee. When the knee is straightened, this tendon is placed under tension, causing the toe to point. This coupling is convenient for running, as it causes extension of all of the leg joints to occur somewhat automatically, making the required spring-off from the toe natural. Thus, a tendon is used to couple the ankle and knee joints of the robotic system, eliminating the need for an active actuator at the ankle.

The second main difference is the type of actuators used. In the prismatic model, all actuators matched the joint type they act upon—revolute actuators at the pelvis and hips and prismatic actuators at the knees. In the articulated model, pneumatic cylinders were used to control the knees. Pneumatic actuators were selected because of their passive energy storage and release abilities, which allow some of the impact energy to be captured, stored, and released during thrusting.

The final difference between the articulated and prismatic models lies in their mass distributions. While the prismatic model was given human mass and inertia values, the articulated model was given mass and inertia values to match a mechanical system constructed of commonly available materials. For example, the legs are constructed out of aluminum square tubing with 3.2 mm wall thickness and 25 mm width and the knee cylinders have a 64 mm bore, 125 mm stroke, and 1.1 kg mass. The full list of parameters is given in Table II.

3.2.1. Steady-state. For the articulated system, the leg thrust could no longer be prescribed to a constant value. Instead, the tristate valve controlling flow to the chambers was fully

https://doi.org/10.1017/S0263574711000166 Published online by Cambridge University Press

Table II. Model parameters for the second simulated system, which are taken from commonly available mechanical materials.

Link	Length (m)	Mass (kg)	Inertia (kg/m^2) (lateral, longitudinal, vertical)
Torso	0.2	12	2, 2, 2
Thigh	0.45	5.6	1.14, 1.14, 0.11
Shank	0.45	1.1	0.22, 0.22, 0.02
Foot	0.21	0.45	0.01, 0.01, 0.01

opened such that the upper chamber had 830 kPa applied and the lower chamber was vented to the atmosphere at 101 kPa. The leg spread angle β_{hip} is corresponds directly to the hip spread angle β_{hip} because the knees are only one DOF. The leg swing angle α_{hip} can be controlled by adjusting both the hip swing angle α_{hip} and the knee swing angle α_{knee}. In order to avoid landing at the singularity of the leg, the knee is flexed to a nominal angle in flight. This leaves the hip to control the leg swing. Since the knee swing angle most directly corresponds to the leg length, it is used to determine when to terminate ground contact. The resulting control laws look remarkably similar to those for the prismatic legged system:

$$\alpha_{\text{hip}}^{\text{fs}} = \alpha_{\text{hip}}^{\text{nom}}\left(1 + k_{sw}^{\text{F}}\text{v}_{\text{F}}^{\text{err}} - k_{sw}^{\text{Z}}\text{p}_{\text{Z}}^{\text{err}}\right), \tag{12}$$

$$\beta_{\text{hip}}^{\text{fs}} = \beta_{\text{hip}}^{\text{nom}}\left(1 + k_{sp}^{\text{L}}\text{v}_{\text{L}}^{\text{err}}\right), \tag{13}$$

$$\alpha_{\text{knee}}^{\text{fs}} = \alpha_{\text{knee}}^{\text{nom}}, \tag{14}$$

$$\alpha_{\text{knee}}^{\text{to}} = \alpha_{\text{knee}}^{\text{nom}}\left(1 + k_{len}^{\text{F}}\left|\text{v}_{\text{F}}^{\text{err}}\right| - k_{len}^{\text{Z}}\text{p}_{\text{Z}}^{\text{err}}\right), \tag{15}$$

where $\alpha_{\text{hip}}^{\text{nom}}$, $\beta_{\text{hip}}^{\text{nom}}$, and $\alpha_{\text{knee}}^{\text{nom}}$ are some preselected leg swing and spread angles at foot-strike, $\alpha_{\text{hip}}^{\text{fs}}$, $\beta_{\text{hip}}^{\text{fs}}$, and $\alpha_{\text{knee}}^{\text{fs}}$ are the desired hip and knee angles at foot-strike adjusted for velocity errors, $\alpha_{\text{knee}}^{\text{to}}$ is the desired knee angle at toe-off, and k_{param}^{dir} is proportional control gain. These adjusted parameters, as well as SS.1, can then be fed into whatever control algorithms are desired to control specific joints. For the results presented in Section 4, simple proportional-derivative control was implemented, with linear gain scheduling to allow performance over a wide operating range.

3.2.2. Acceleration. The accelerating heuristics given in Section 2.1 can also be converted into control laws. For acceleration, the equations governing the four control parameters become

$$\alpha_{\text{hip}}^{\text{fs}} = \alpha_{\text{hip}}^{\text{accel}}, \tag{16}$$

$$\beta_{\text{hip}}^{\text{fs}} = \beta_{\text{hip}}^{\text{nom}}\left(1 + k_{sp}^{\text{L}}\text{v}_{\text{L}}^{\text{err}}\right), \tag{17}$$

$$\alpha_{\text{knee}}^{\text{fs}} = \alpha_{\text{knee}}^{\text{accel}}, \tag{18}$$

$$\alpha_{\text{knee}}^{\text{to}} = \alpha_{\text{knee}}^{\text{max}}, \tag{19}$$

where $\alpha_{\text{knee}}^{\text{max}}$ is the maximum possible knee extension.

Despite the stark differences between the prismatic and articulated systems, the control laws are actually remarkably similar, as is shown in Fig. 3.

		Steady-state	Accelerating
Prismatic	$\alpha_{\text{hip}}^{\text{fs}}$	$\alpha_{\text{hip}}^{\text{nom}}\left(1 + k_{sw}^{\text{F}}\text{v}_{\text{F}}^{\text{err}} - k_{sw}^{\text{Z}}\text{p}_{\text{Z}}^{\text{err}}\right)$	0^o
	$\beta_{\text{hip}}^{\text{fs}}$	$\beta_{\text{hip}}^{\text{nom}}\left(1 + k_{sp}^{\text{L}}\text{v}_{\text{L}}^{\text{err}}\right)$	$\beta_{\text{hip}}^{\text{nom}}\left(1 + k_{sp}^{\text{L}}\text{v}_{\text{L}}^{\text{err}}\right)$
	$\ell_{\text{leg}}^{\text{fs}}$	$\ell_{\text{leg}}^{\text{nom}}$	$\ell_{\text{leg}}^{\text{nom}}\left(1 - k_{len}^{\text{F}}\text{v}_{\text{F}}^{\text{err}}\right)$
	$\ell_{\text{leg}}^{\text{to}}$	$\ell_{\text{leg}}^{\text{nom}}\left(1 + k_{len}^{\text{F}}\left\|\text{v}_{\text{F}}^{\text{err}}\right\| - k_{len}^{\text{Z}}\text{p}_{\text{Z}}^{\text{err}}\right)$	$\ell_{\text{leg}}^{\text{max}}$
Articulated	$\alpha_{\text{hip}}^{\text{fs}}$	$\alpha_{\text{hip}}^{\text{nom}}\left(1 + k_{sw}^{\text{F}}\text{v}_{\text{F}}^{\text{err}} - k_{sw}^{\text{Z}}\text{p}_{\text{Z}}^{\text{err}}\right)$	$\alpha_{\text{hip}}^{\text{accel}}$
	$\beta_{\text{hip}}^{\text{fs}}$	$\beta_{\text{hip}}^{\text{nom}}\left(1 + k_{sp}^{\text{L}}\text{v}_{\text{L}}^{\text{err}}\right)$	$\beta_{\text{hip}}^{\text{nom}}\left(1 + k_{sp}^{\text{L}}\text{v}_{\text{L}}^{\text{err}}\right)$
	$\alpha_{\text{knee}}^{\text{fs}}$	$\alpha_{\text{knee}}^{\text{nom}}$	$\alpha_{\text{knee}}^{\text{accel}}$
	$\alpha_{\text{knee}}^{\text{to}}$	$\alpha_{\text{knee}}^{\text{nom}}\left(1 + k_{len}^{\text{F}}\left\|\text{v}_{\text{F}}^{\text{err}}\right\| - k_{len}^{\text{Z}}\text{p}_{\text{Z}}^{\text{err}}\right)$	$\alpha_{\text{knee}}^{\text{max}}$

Fig. 3. Comparison of control laws for prismatic and articulated for steady-state running and accelerating.

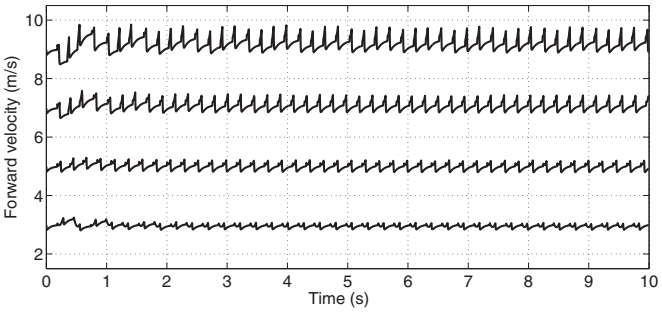

Fig. 4. Steady-state running of the prismatic legged system at 3, 5 , 7 , and 9 m/s.

4. Results

In order to test the heuristics and control laws developed above, a dynamic simulation was created of both systems. This was done using the method outlined in ref. [16]. The symbolic manipulator AutoLev was used to create the equations of motion of the system, and these equations were imported into a dynamic simulator in C++ that uses a variable step Runge–Kutta–Merson algorithm for numerical integration (see Lance[17] for details).

For this simulation, two key assumptions were made. First, it was assumed that the friction between the ground and the foot was sufficient at all times to prevent slipping. This assumption is validated by the fact that the highest required coefficient of friction for the results presented here was $\mu_{\text{max}} < 2$, while observed coefficients of static friction between a rubber foot sole and a steel ground plate fall in the range of 3–10.[18] The other main assumption is that all collisions are inelastic. Collisions are modeled using the generalized impulse-momentum method.[19] The decision to model collisions as inelastic is based on the observation that, in biologic systems performing dynamic gaits, the kinetic energy in the foot is deliberately sacrificed to maintain inelastic collisions.[20]

4.1. Simulated prismatic system

The steady-state controller was tested at speeds across an operating range of 2 to 10 m/s. Figure 4 shows the system COM forward velocity at commanded velocities of 3, 5, 7, and 9 m/s. While there is initially some observable variation,

https://doi.org/10.1017/S0263574711000166 Published online by Cambridge University Press

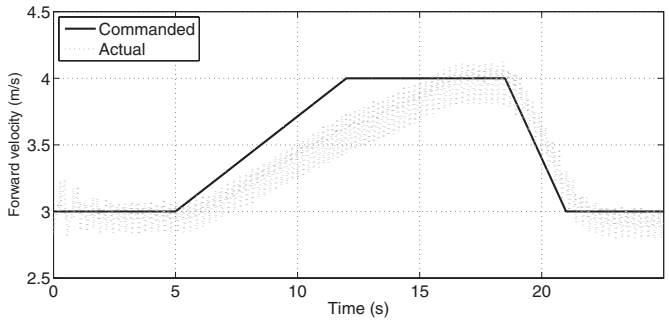

Fig. 5. Low-rate acceleration and deceleration under the steady-state controller.

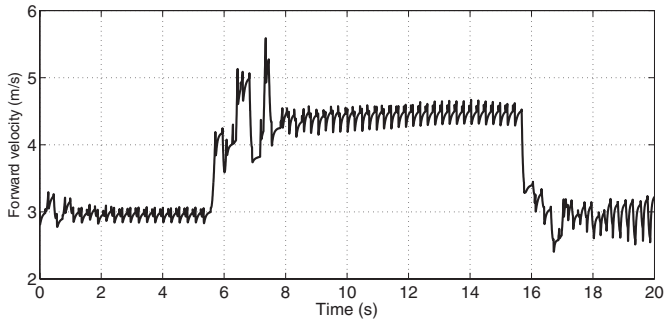

Fig. 6. High-rate acceleration and deceleration of the prismatic legged system under the acceleration controller.

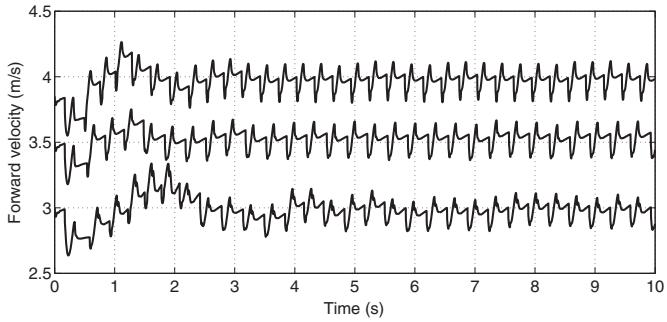

Fig. 7. Steady-state running of the articulated legged system at 3.0, 3.5 , and 4.0 m/s.

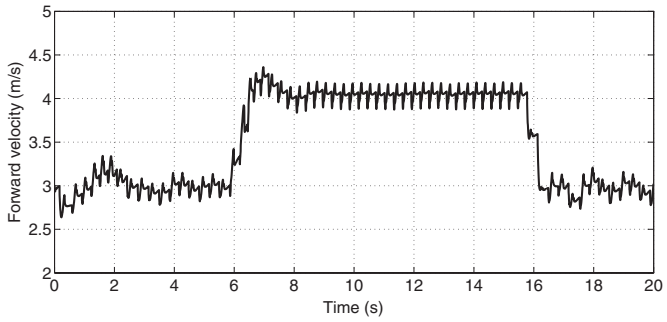

Fig. 8. High-rate acceleration and deceleration of the articulated legged system under the acceleration controller.

especially for higher velocities, the system quickly settles into a steady limit cycle.

Since the steady-state control laws in Section 3 take into account velocity errors, a first attempt at acceleration is made by continually increasing the desired velocity. This produces stable acceleration for low-rate increases, below a few percent per stride, as shown in Fig. 5. During acceleration, the commanded forward velocity increases much more quickly than the actual forward velocity, while during deceleration the commanded and actual velocity match more closely.

For higher rates of acceleration, the steady-state controller leads to unstable results after several strides. Using the heuristics specifically developed for high-rate acceleration presented in Section 2.1, a stable acceleration is produced, as seen in Fig. 6. The biped accelerates in two steps, from a 3 m/s run to a 4.5 m/s run, and then a short while later decelerates back to 3 m/s. It is worth noting that the system does not anticipate acceleration or deceleration, so during acceleration the strong forward thrust causes significant body pitch, which takes a few steps to fix. This is seen in the high degree of variation in the steps immediately following the acceleration and deceleration.

4.2. Simulated articulated system

For the articulated system, the pneumatic cylinders were modeled using a first-order approximation of the model presented in Shen and Goldfarb.[21] The steady-state controller was unable to produce speeds higher than $\approx 4.5\,m/s$. This is a direct result of the limited actuator power in the knees, constrained by the 64 mm bore of the cylinder and the high-pressure input of 830 kPa. Figure 7 shows the system COM forward velocity at commanded velocities of 3.0, 3.5, and 4.0 m/s. Again, there is initially some observable variation, but this quickly settles out to a steady limit cycle.

Figure 8 shows the articulated legged system undergoing acceleration and deceleration by using the control laws developed in Section 3.2.

4.3. Experimental articulated system

A physical system was constructed in order to experimentally test the heuristics and associated control laws for steady-state running. This system, shown in Fig. 9, is constructed according to the design of the articulated system described in Section 3.2, with two important distinctions. First, the experimental system is constrained to motion in the sagittal plane by means of a boom arm. Second, the torso is free to rotate about the hip in the pitch plane but is attached to a vertical axis by means of a pneumatic cylinder, as shown in Fig. 9. The valves for this cylinder are locked in a position partially opened to atmosphere. The result of this setup is a measure of skyhook damping on the torso pitch, as well as a nonlinear spring torque during high pitch rates. This setup is chosen due to observations that controlling the pitch of the torso played a substantial role in both the stability of Raibert's biped[2] and in the eventual loss of control of RABBIT.[6] In order to execute a run in the limited confines of the laboratory, a 3 m long treadmill is placed under the biped.

Using the control algorithm developed in Section 3.2, a stable steady-state run was achieved at $v_F^{des} = 1\,m/s$, producing the forward and vertical velocity of the center of the hip axis shown in Fig. 10. Examining the forward velocity yields two significant observations. The first is that the system

https://doi.org/10.1017/S0263574711000166 Published online by Cambridge University Press

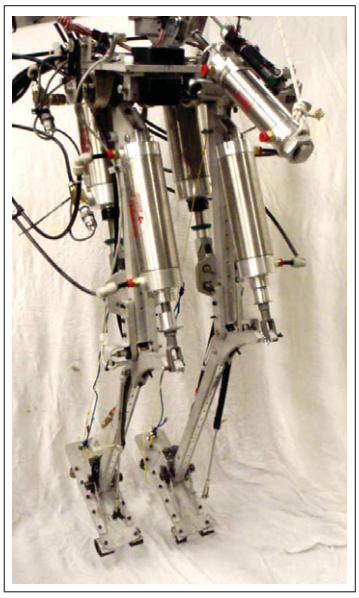

Fig. 9. Robotic biped used for steady-state running experiments. The cylinder extending from the torso is used to apply skyhook damping.

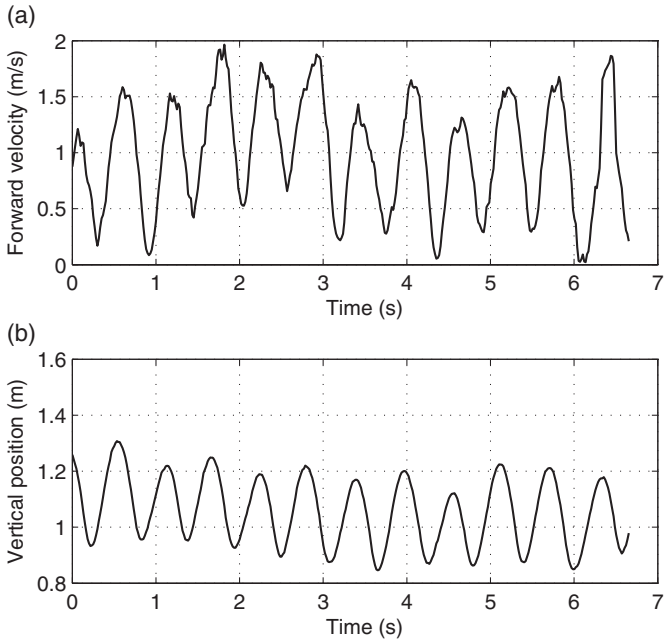

Fig. 10. (a) Forward velocity and (b) vertical position of the center of the hip axis of the experimental system during steady-state running at $v_F^{des} = 1$ m/s with a semiconstrained torso.

behaves as desired, running stably with a forward velocity of $v_F^{act} \approx 1\,m/s$. This demonstrates that both the steady-state heuristics developed in Section 2.1 and the specialized control laws developed in Section 3.2 are appropriate for steady-state running, with two exceptions: SS.2 cannot be validated because it is unknown what contribution the semiconstrained torso plays in positioning the swing leg during flight, and SS.3 cannot be validated because the experimental system is constrained to the sagittal plane.

The second significant observation about the forward velocity of the center of the hip axis of the experimental system is that it varies much more than the simulation predicts. For the simulated system running at $v_F^{des} = 3\,m/s$, Fig. 7 shows a variation of $\approx 0.25\,m/s$, or 8% of v_F^{des}. However, for the experimental system running at $v_F^{des} = 1\,m/s$, Fig. 10 shows a variation of $\approx 1.4\,m/s$, or 140% of v_F^{des}.

There are two causes of this variation: the pneumatic cylinder used to impose the semiconstraint on the torso pitch and the friction in the treadmill. As mentioned previously, a pneumatic cylinder is attached between the boom and a point on the torso with its intake valves partially opened. When the torso pitches a spring force is developed in the cylinder. The boom and biped have inertias of 49 kg/m^2 and 98 kg/m^2 about the pivot point of the boom in the horizontal plane. Thus, when a spring force is applied between the two, the biped will be pulled back toward the boom about half as much as the boom is pulled forward toward the biped, contributing to the velocity variation as shown in Fig. 10.

The other cause of the variation in the forward velocity is the friction in the treadmill, which consists of a rubber tread sliding over a sheet of plywood. When the foot strikes the treadmill, the normal force, and therefore the friction force, between the tread and the support wood drastically increases, causing the treadmill to decelerate. Since the torso is moving approximately vertically (i.e., running in place over a horizontally translating floor), the forward speed of the robot is determined largely by the speed of the tread. When the tread drastically decelerates, it is analogous to the robot drastically decelerating, as seen in Fig. 10.

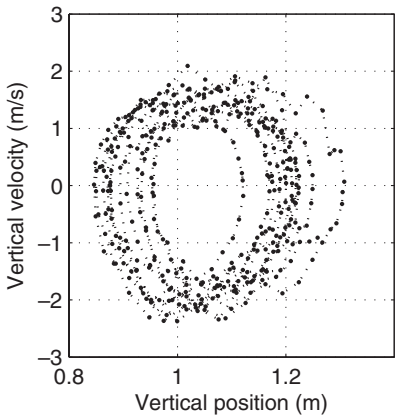

Fig. 11. Phase plot for vertical position of the center of the hip axis for the experimental system during steady-state running at $v_F^{des} = 1\,m/s$ with a semiconstrained torso, demonstrating convergence to stable limit cycles.

The phase plot of the vertical position of the center of the hip axis is shown in Fig. 11. The presence of a limit cycle again confirms that a stable run is achieved.

5. Discussion

As previously mentioned, one of the strengths of heuristic control is the applicability of a single set of heuristics to a wide range of systems. This is clearly illustrated here, when the same set of seven simple heuristics produce stable steady-state and accelerated running in two very disparate

https://doi.org/10.1017/S0263574711000166 Published online by Cambridge University Press

systems. The prismatic legged system has human parameters, which means that the torso has a relatively high inertia, allowing the leg to be easily positioned during flight without a gross sacrifice of torso pitch and roll. This system also had essentially perfect actuators with no limits on their thrusting abilities. Under such an idealized system, it is not entirely surprising that the heuristics are able to produce stable results.

The articulated legged system, however, had none of these luxuries: the torso was relatively low inertia, with approximately 50% of the system mass in the legs, and very limited actuators. Both systems also had the same number of active DOFs, althouth the articulated legged system has four more DOFs than the prismatic legged system. Yet, despite these complications, the same seven heuristics produced stable results on the articulated legged system as well. The heuristics are general enough that it is insensitive to the incredible differences in system architectures. This stands in stark contrast to other control methods, such as model-based control, in which even minor changes in system architecture can require a completely new controller.

The results in Figs. 5 and 6 also illustrate the important point that acceleration and deceleration are fundamentally separate from steady-state running. This is not altogether surprising on an intuitive level, though it could be argued that since the steady-state heuristics and control laws take into account the deviation from the desired velocity, they should be able to produce acceleration and deceleration. However, high-rate acceleration and deceleration require significant energy additions and subtractions, which the steady-state controller is insufficient for. When using the steady-state controller for acceleration, there is an exchange of vertical energy for forward energy, manifested in a decrease of hopping height to create an increase in forward velocity. If the hopping height is reduced too much, the system "trips", snagging the swing foot on the ground. During deceleration, the hopping height is increased as the forward velocity decreases, which is much less likely to destabilize the system. By using heuristics dedicated specifically to acceleration and deceleration, the system is able to anticipate the required change in energy and thus avoids these effects.

As demonstrated, the heuristics developed here are applicable to a wide range of systems. A simple procedure to implement them on a new system is given here. First, the relevant parameters corresponding to effective leg length and foot forward and lateral position must be identified. Each of the heuristics in Section 2.1 are then considered and used to adjust these parameters. For example, SS.4 dictates the forward position of the foot at foot-strike according to the forward velocity error. By considering each heuristic, formulas for adjusting the relevant parameters are derived. Any desired control laws can then be used to ensure that these parameters achieve their target values.

6. Conclusion

A set of heuristics based on observations of biologic systems and physical principles was developed for both steady-state and accelerated running. These heuristics are simple and easily applied to bipedal robots. Given two very different systems, one with prismatic legs and the other with articulated legs, the heuristics were converted into simple proportional control laws. These were implemented in simulation to produce stable steady-state running at a range of speeds on both systems. Four of the six steady-state heuristics were also validated on a planar experimental system with a semiconstrained torso. Using the acceleration control laws, high-rate acceleration and deceleration were achieved.

Acknowledgments

The authors gratefully acknowledge funding provided by the National Science Foundation grant CMMI-0825364.

References

1. A. J. McClung, M. R. Cutkosky and J. G. Cham, "Rapid Maneuvering of a Biologically Inspired Hexapedal Robot," *Proceeding of 2004 ASME International Mechanical Engineering Congress and Exposition*, Anaheim, CA (Nov. 2004), IMECE2004-61150.
2. M. Raibert, *Legged Robots that Balance* (MIT Press, Cambridge, MA, 1986).
3. R. Playter, M. Buehler and M. Raibert, "Bigdog," volume 6230, *Proceeding of the SPIE*, Orlando, FL (2006), p. 62302O.
4. M. Hirose and K. Ogawa, "Honda humanoid robots development," *Phil. Trans. R. Soc.* A **365**(1850), 11–19 (2007).
5. R. M. Alexander, "Optimization and gaits in the locomotion of vertebrates," *Physiol. Rev.* **69**(4), 1199–1227 (1989).
6. C. Chevallereau, G. Abba, Y. Aoustin, F. Plestan, E. R. Westervelt, C. C. de Wit and J. W. Grizzle, "Rabbit: A testbed for advanced control theory," *IEEE Control Syst. Mag.* **23**(5), 57–79 (2003).
7. D. W. Marchhefka and D. E. Orin, "Fuzzy Control of Quadrupedal Running," *Proceeding of 2000 IEEE International Conference on Robotics and Automation*, volume 3, San Francisco, CA (Apr. 2000), pp. 3063–3069.
8. M. A. Lewis, M. J. Hartmann, R. Etienne-Cummings and A. H. Cohen, "Control of a robot leg with an adaptive VLSI CPG chip," *Neurcomputing* **38**(40), 1409–1421 (2001).
9. G. Endo, J. Morimoto, J. Nakanishi and G. Cheng, "An Empirical Exploration of a Neural Oscillator for Biped Locomotion Control," *Proceeding of 2004 IEEE Intetnational Conference on Robotics and Automation*, New Orleans, LA (Apr. 2004), pp. 3036–3042.
10. R. Blickhan, "The spring-mass model for running and hopping," *J. Biomech.* **22**(11/12), 1217–1227 (1989).
11. M. E. Abdallah and K. J. Waldron, "A Physical Model and Control Strategy for Biped Running," *Proceeding of 2007 IEEE International Conference on Robotics and Automation*, Roma, Italy (Apr. 2007), pp. 3982–3988.
12. A. Goswami, B. Espiau and A. Keramane, "Limit cycles in a passive compass gait biped and passivity-mimicking control laws," *Auton. Robot* **4**(3), 273–286 (1997).
13. P. Leva, "Adjustments to zatsiorsky-seluyanov's segment inertia parameters,", *J. Biomech.* **29**(9), 1223–1230 (1996).
14. M. E. Abdallah, Mechanics Motivated Control and Design of Biped Running *Ph.D. Thesis* (Stanford University, Stanford, CA, 2007).
15. A. D. Perkins and K. J. Waldron, "The Effects of Ankle Stiffness on Articulated Planar Hopping," *Proceeding of 2008 CISM-IFToMM Symposium on Robot Design, Dynamics, and Control*, Tokyo, Japan (Jul. 2008), pp. 521–527.
16. A. D. Perkins, M. E. Abdallah, P. Mitiguy and K. J. Waldron, "A Unified Method for Simulating Multi-Body Systems Subject to Stick-Slip Friction and Intermittent Contact," *Proceeding of IEEE International Conference on Intelligent Robotics and Systems*, Nice, France (Sep. 2008), pp. 2311–2316.
17. G. N. Lance, *Numerical Methods for High-Speed Computers* (Iliffe & Sons, London, UK, 1960).

18. V. Castelli, *Marchks' Standard Handbook for Mechanical Engineers*, 10th ed., Chap. 3.2 (Friction McGraw Hill, New York, NY, 1996).
19. T. Kane and D. Levinson, *Dynamics: Theory and Applications* (McGraw-Hill, New York, NY, 1985).
20. K. J. Waldron, J. Estremera, P. J. Csonka and S. P. N. Singh, "Thinking about bounding and galloping using simple models," *Proceeding of 2008 International Conference on Climbing and Walking Robots*, Singapore (Sep. 2008), pp. 445–453.
21. X. Shen and M. Goldfarb, "Independent stiffness and force control of pneumatic actuators for contact stability during robot manipulation," *Proceeding of 2005 IEEE International Conference on Robotics and Automation*, Barcelona, Spain (Apr. 2005), pp. 2697–2702.

https://doi.org/10.1017/S0263574711000166 Published online by Cambridge University Press